JOURNAL OF SOLID STATE CHEMISTRY 67, 109–121 (1987)

Synthesis, Characterization, and Magnetic Properties of Mixed-Valence Europium–Ammonia Intercalation Compounds of Titanium Disulfide*

S. P. HSU AND W. S. GLAUNSINGER†

Department of Chemistry, Arizona State University, Tempe, Arizona 85287

Received March 17, 1986; in revised form June 23, 1986

Europium–ammonia intercalation compounds of titanium disulfide have been synthesized by reaction of Eu–NH_3 solutions with TiS_2, characterized by thermogravimetric analysis and powder X-ray diffraction, and investigated by electron paramagnetic resonance, magnetization, and magnetic susceptibility measurements. These materials crystallize in a 3*R*-type structure in which every layer is occupied by intercalated species. The intercalation of NH_3 is accompanied by the formation of NH_4^+ until a critical electron concentration of 0.22 mole el/mole TiS_2 have been transferred to the TiS_2 conduction band. Although Eu^{3+} is the predominant Eu species for $x > 0.001$, Eu^{2+} is also formed, possibly from the reduction of Eu^{3+} in the van der Waals gap. These mixed-valence compounds are best described by the formulas $(Eu^{3+})_{x'}(Eu^{2+})_{x''}(NH_4^+)_{y'}(NH_3)_{y''}TiS_2^{(3x'+2y''+y')-}$ for $3x' + 2x'' + y' < 0.22$ and $(Eu^{3+})_{x'}(Eu^{2+})_{x''}(NH_3)_{y''}TiS_2^{(3x'+2x'')-}$ for $3x' + 2x'' \geq 0.22$.

Introduction

The lamellar transition metal disulfides (TS_2) have been one of the most popular hosts for practicing intercalation chemistry due to the intriguing properties and practical applications of these low-dimensional materials (*1–8*). Basically, intercalation of TS_2 involves the vertical separation of the [S–*T*–S] layers along the **c** axis accompanied by insertion of guest species into unoccupied interstitial sites in the van der Waals gap. In this process, host–host interactions are replaced by energetically more favorable guest–host and guest–guest interactions. A wide variety of chemical species can be intercalated into TS_2 hosts, including organic and inorganic Lewis bases, organometallic complexes, electropositive metals, and transition metals (*1–3*).

Ammonia is the simplest Lewis base that can be intercalated into TS_2 and has been the subject of numerous investigations (*9–23*). The most recent work on ammoniated TiS_2 has revealed that NH_3 is oxidized to form NH_4^+, which is intercalated into TiS_2 in addition to neutral NH_3 (*20, 22, 23*). The formula for these materials can be written $(NH_4^+)_{y'}(NH_3)_{y''}TiS_2^{y'-}$, and they consist of planar arrays of NH_4^+ sandwiched between polyanionic $[TiS_2]^{y'-}$ sheets. NH_4^+ is formed up to the limiting composition $y' = 0.22 \pm 0.02$, and one electron is donated to the host TiS_2 conduction band per NH_4^+ ion, which renders these compounds metallic. Apparently, at this critical electron concentration the chemical potentials of the intercalant and TiS_2 are equal, so that no further NH_3 oxidation occurs. It is also possible to

* This research was supported by NSF Grant DMR 82-15315.

† To whom correspondence should be addressed.

0022-4596/87 $3.00

cointercalate Li and NH_3 into TiS_2 by immersing the host in Li–NH_3 solutions, and the resulting intercalation compounds can be formulated as $Li_x^+(NH_4^+)_{y'}(NH_3)_{y''}TiS_2^{(x+y')-}$ for $0 \leq x \leq 0.20$ (*22, 24*). In these materials, NH_4^+ and Li^+ are analogous in terms of charge transfer, which is accomplished by initial ionization of Li to Li^+ followed by oxidation of sufficient NH_3 to NH_4^+ to achieve the critical electron concentration of 0.22 mole of electrons per mole of TiS_2, i.e., $x + y' = 0.22$.

Since Li–NH_3 solutions intercalate rapidly into TiS_2, it is reasonable to expect Eu–NH_3 solutions to intercalate in a similar fashion to form the intercalation compounds $Eu_x(NH_3)_yTiS_2$, where x and y denote the overall europium and ammonia compositions, respectively. Indeed, a few Eu–NH_3 intercalation compounds of NbS_2 and MoS_2 have been reported in the literature (*25, 26*). Such Eu–NH_3 intercalation compounds would presumably have the advantage of using the natural paramagnetic probe Eu^{2+} to investigate the site symmetry and magnetic interactions in these materials, since Eu^{2+} is the only cation present in Eu–NH_3 solutions (*27, 28*). In agreement with this expectation, previous magnetic studies of Eu–NH_3 intercalation compounds of NbS_2 and MoS_2 have indicated the presence of Eu^{2+} (*25, 26*). The magnetic properties of the former compounds are complex and exhibit paramagnetism, ferromagnetism, and possibly superparamagnetism (*25*).

In this work, we have elucidated the nature of the intercalated species in Eu–NH_3 intercalation compounds of TiS_2 by carefully synthesizing these materials at low temperatures, characterizing them by thermogravimetric analysis (TGA) and powder X-ray diffraction, and investigating their magnetic properties using electron paramagnetic resonance (EPR) an SQUID magnetometry. We have found that NH_3, NH_4^+, Eu^{2+}, and Eu^{3+} are present in the van der Waals gap, with Eu^{3+} being the predominant valence state of Eu.

Experimental

All Eu–NH_3 intercalation compounds were prepared using highly stoichiometric TiS_2 having the formula $Ti_{1.0021\pm0.0010}S_2$(*22*). All glassware was cleaned using a HF cleaning solution consisting of 90 ml of 48% hydrofluoric acid, 330 ml of 70% nitric acid, 400 ml of distilled water, and 20 g of Alconox. Glassware was exposed to this solution for about 3 min, rinsed several (≈25) times with distilled water, and finally rinsed a few (≈5) times with deionized, doubly distilled water. High-purity Eu was obtained from Ames Laboratory at Iowa State University. The preparation of Eu–NH_3 solutions has been described elsewhere (*28*). The intercalation reaction was carried out by reacting polycrystalline TiS_2 (≈80 mesh) with liquid Eu–NH_3 solutions in an h-cell maintained below 240 K to minimize solution decomposition reactions. The Eu–NH_3 solutions originally had the characteristic blue color due to solvated electrons (*28*), which gradually disappeared as the Eu intercalated into TiS_2. The intercalation reaction was considered complete when the Eu–NH_3 solution became colorless. The reaction times increased with Eu concentration, and at the low temperature necessary to minimize decomposition, ranged from several days to several weeks. After the reaction was complete, the excess NH_3 was poured into the opposite leg of the h-cell, and the leg containing the sample was sealed off. The samples were very sensitive to air and moisture and were handled whenever possible in a helium-filled Vacuum Atmospheres Model MO-40-1H Dry Train glovebox containing less than 1 ppm water and oxygen and only removed from the glovebox in sealed containers.

The NH_4^+ and NH_3 compositions were determined by TGA using a modified

Perkin-Elmer TGS-2 system having an ultimate 0.1 μg sensitivity and 0.01% weight resolution using the procedure described previously (*20*). The temperature was increased from 25 to 230°C at rates of 1–2°C/min. For a typical sample mass of 5 mg, mass changes of 4 μg can be resolved routinely. The overall NH_4^+ and NH_3 compositions could be measured reliably to ± 0.01 by TGA.

Phase and structural information were obtained by powder X-ray diffraction. Patterns were recorded at ambient temperature using Ni-filtered Cu$K\alpha$ radiation. Samples were loaded into 0.3-mm Pyrex capillaries in the glovebox and sealed before loading them into a calibrated Debye-Scherrer camera. The exposure time for all intercalation compounds was about 24 hr.

Paramagnetic species were investigated by EPR and SQUID magnetometry. EPR spectra were recorded in the range 4.2–300 K using a Bruker-IBM ER 200D spectrometer operating at X band. EPR samples were loaded into high-purity, 3-mm-i.d. quartz tubes in the glovebox and then sealed on a high-vacuum line to prevent contamination. Magnetic measurements were performed in the ranges 0–50 kG and 5–300 K using a SHE Model VTS-905 SQUID magnetometer. The procedure has been given elsewhere (*20*).

Results and Discussion

1. Synthesis

There are several factors that are important in the preparation of these intercalation compounds. First, high-purity Eu should be used because impurities, especially the transition metals, will catalyze the decomposition of Eu–NH_3 solutions according to the reaction $Eu^{2+} + 2e_s^- + 2NH_3 \rightarrow Eu(NH_2)_2 + H_2$, where e_s^- represents the solvated electron (*23*). Moreover, the $Eu(NH_2)_2$ decomposition product itself further catalyzes the decomposition reaction, so that this reaction is autocatalytic. Second, the glassware to which the Eu–NH_3 solutions are exposed should be thoroughly cleaned with a HF-based cleaning solution to prevent decomposition catalyzed by the surface of the glassware. Third, the intercalation reaction should be conducted at low temperatures to minimize decomposition of the Eu–NH_3 solutions induced by the host TiS_2. The decomposition reaction is probably catalyzed by coordinately unsaturated Ti at the edges of the TiS_2 particles. The occurrence of this reaction is evidenced by the appearance of yellow-orange $Eu(NH_2)_2$ at the surface of the TiS_2 particles. Solution decomposition is noticeable above about 240 K, which is the boiling point of liquid NH_3. Reaction temperatures in the range 220–240 K are effective in minimizing decomposition, with the lower temperatures requiring long reaction times (weeks to months). Fourth, TiS_2 should be as stoichiometric as possible to minimize the time required for the intercalation reaction, since excess Ti in the van der Waals gap reduces dramatically the intercalation rate. The time required for complete NH_3 intercalation of TiS_2 at 20°C was slightly less than 2 hr, which is the fastest intercalation time reported to date (*22, 29*) and attests to the near stoichiometry of the host. Finally, the Eu–NH_3 intercalation compounds should be stored at low temperatures ($\lesssim$240 K) and handled in an inert-atmosphere glovebox to minimize decomposition and contamination by air and moisture, respectively. If the above precautions are taken, then it is possible to prepare high-quality Eu–NH_3 intercalation compounds of TiS_2 suitable for detailed physical measurements.

2. Characterization

Typical deintercalation curves for $Eu_x(NH_3)_yTiS_2$ intercalation compounds are displayed in Figs. 1 and 2. From the mea-

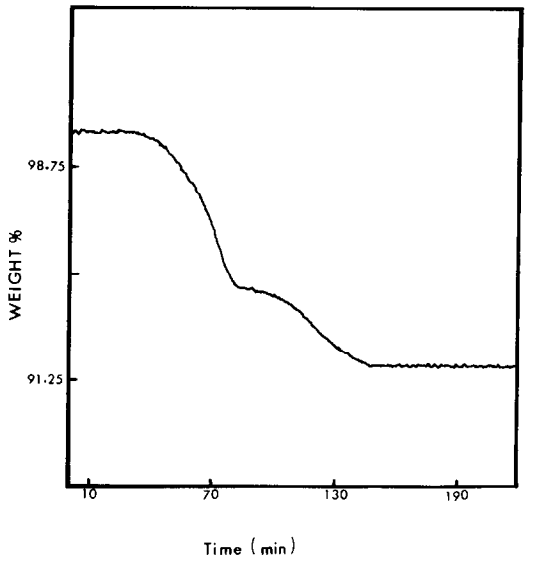

FIG. 1. Typical TGA deintercalation curve for $Eu_{0.014}(NH_3)_yTiS_2$. The heating rate is 2°C/min.

sured mass loss, the NH_3 and NH_4^+ compositions could be determined with high precision. The low- and high-temperature steps observed in Fig. 1 are due to the thermal deintercalation of NH_3 and NH_4^+, respectively. The deintercalation of the latter species occurs at higher temperatures due to the stronger ionic attractive interactions between NH_4^+ and the negatively charged TiS_2 layers and, furthermore, is accompanied by the chemical reaction $NH_4^+ \rightarrow NH_3 + \frac{1}{2}H_2$ (*20, 22*). Such two-step deintercalation curves were found for relatively low Eu contents ($x \lesssim 0.07$). In contrast, for higher Eu composition ($x \gtrsim 0.07$), only one step is resolved in the thermal deintercalation curve, as shown in Fig. 2. This step is due to the deintercalation of NH_3, which occurs over approximately the same temperature range as found in samples having low Eu contents (see Fig. 1).

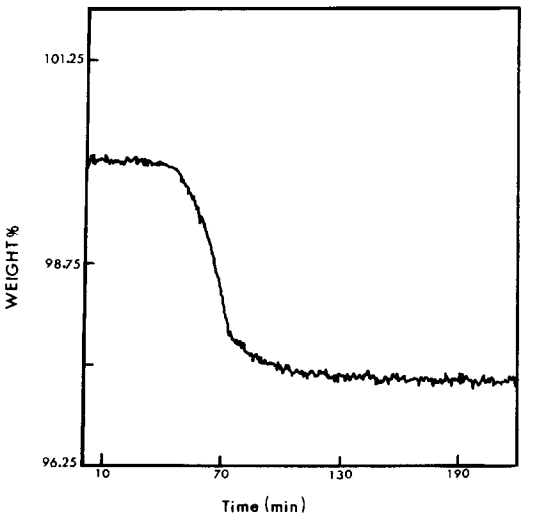

FIG. 2. Typical TGA deintercalation curve for $Eu_{0.170}(NH_3)_yTiS_2$. The heating rate is 2°C/min.

The NH_4^+ and NH_3 compositions of $Eu_x(NH_4^+)_{y'}(NH_3)_{y''}$ TiS_2 intercalation compounds determined by TGA are given in Table I. For the two lowest values of x, the NH_4^+ composition is equal within experimental error to that required in ammoniated and lithium-ammoniated TiS_2 (*20, 22, 24*) to satisfy the electronic requirements of the host TiS_2 ($y' = 0.22 \pm 0.02$). However, for $x = 0.066$ there is a sharp reduction in the NH_4^+ content, and for $x \geq 0.077$ no NH_4^+ could be observed, even at the highest sensitivities of the TGA system. As found for

TABLE I

NH_4^+ AND NH_3 COMPOSITIONS FOR $Eu_x(NH_4^+)_{y'}(NH_3)_{y''}TiS_2$ INTERCALATION COMPOUNDS DETERMINED BY TGA

x^a	y'	y''
0.001	0.23	0.33
0.007	0.20	0.38
0.014	0.19	0.40
0.066	0.08	0.26
0.077	0	0.19
0.107	0	0.29
0.170	0	0.18
0.274	0	0.47

[a] The Eu composition is nominal. The precision of the NH_4^+, NH_3 compositions is ±0.02.

the Li–NH_3 intercalates of TiS_2, (*22, 24*), the reason for this behavior is that the intercalation of Eu is relatively rapid compared to NH_3 and is accompanied by electronic charge transfer to the TiS_2 conduction band, which reduces the amount of NH_4^+ that must be formed to provide the TiS_2 conduction band with the requisite 0.22 ± 0.02 mole el/mole TiS_2. Beyond this electronic concentration, no further oxidation of NH_3 to NH_4^+ is necessary, and any additional electrons transferred to TiS_2 originate from the ionization of Eu. Therefore, in principle it should be possible to derive the oxidation state of Eu from the lowest Eu concentration at which no NH_4^+ is formed, since at this Eu concentation $zx_l \simeq 0.22$, where z is the charge of the Eu cation. Taking $x_l \simeq 0.077$ from Table I, we find $z \simeq 2.9$, which suggests that Eu is in the trivalent, rather than in the divalent, state found in the starting Eu–NH_3 solutions (*27, 28*). Therefore, it appears that these intercalation compounds can be described approximately by the formulas $(Eu^{3+})_{x'}(NH_4^+)_{y'}(NH_3)_{y''}TiS_2^{(3x'+y')-}$ for $3x' + y' < 0.22$. This result indicates that the redox potential of the Eu^0/Eu^{3+} couple is more negative than the redox potentials of the couples NH_3/NH_4^+, Eu^0/Eu^+, Eu^0/Eu^{2+}, Eu^+/Eu^{2+}, and Eu^{2+}/Eu^{3+}. The existence and concentration of Eu^{3+} can be determined more quantitatively from magnetic measuremnts, as demonstrated in the next section.

The X-ray diffraction patterns of all Eu–NH_3 intercalation compounds could be indexed using hexagonal cells arranged in a three-layer, 3*R*-type structure in which every layer is occupied by intercalated species. Least-squares refinements were performed on the *d* values to derive precise cell constants. An example of the agreement obtained between the observed and calculated *d* values is given in Table II for $Eu_{0.17}(NH_3)_{0.18}TiS_2$. Many of the X-ray reflections were relatively weak, which necessitated relatively long exposure times.

TABLE II

POWDER DIFFRACTION DATA FOR $Eu_{0.17}(NH_3)_{0.18}TiS_2$

hkl	d_{obs} (Å)	d_{cal} (Å)[a]	Intensity
0 0 3	8.336	8.304	m
1 0 1	2.944	2.916	w
0 1 2	2.885	2.888	m
0 1 5	2.590	2.595	s
0 1 8	2.145	2.147	w
1 1 0	1.710	1.712	s
1 1 3	1.670	1.677	w
2 0 2	1.472	1.472	w
0 2 4	1.444	1.442	w
2 0 5	1.423	1.421	w
2 0 8	1.338	1.338	w
0 0 21	1.185	1.186	w
1 2 5	1.093	1.093	vw
1 2 8	1.054	1.055	vw
3 0 0	0.987	0.988	vw

[a] The cell constants are **a** = 3.424 Å and **c** = 24.91 Å. The uncertainties in **a** and **c** are ±0.005 and ±0.01 Å, respectively.

The diffuse nature of some of the lines is probably due to the disorder inherent in these nonstoichometric intercalation compounds. Also, for $Eu_{0.0001}(NH_3)_{0.55}TiS_2$ and $Eu_{0.107}(NH_3)_{0.29}TiS_2$ a very weak diffuse line having $d = 7.4$ Å was observed. This line could be indexed to a stage II phase in which every other van der Waals gap is occupied and has been observed previously in both ammoniated and lithium-ammoniated TiS_2 (*20, 22*).

The cell parameters for $Eu_x(NH_3)_yTiS_2$ intercalation compounds are summarized in Table III. The expansion of the **c** axis upon intercalation by 3.0–3.2 Å for all compounds except $Eu_{0.17}(NH_3)_{0.18}TiS_2$ indicates that the larger NH_4^+ and NH_3 are the species responsible for the expansion, since the radii of Eu^{2+}, Eu^{3+}, NH_4^+, and NH_3 are 1.10, 0.95, 1.43 (*30*), and 1.67 (*31*), respectively. The smaller expansion for $Eu_{0.17}(NH_3)_{0.18}TiS_2$ probably reflects its lower NH_3 and higher Eu contents as well as stronger ionic bonding between Eu^{3+} and

TABLE III

CELL PARAMETERS FOR $Eu_x(NH_3)_yTiS_2$ INTERCALATION COMPOUNDS DETERMINED BY POWDER X-RAY DIFFRACTION

x	a[a]	c[b]	Δc[c]
0.001	3.415	26.71	3.2
0.007	3.416	26.72	3.2
0.014	3.413	26.16	3.0
0.066	3.419	26.56	3.2
0.077	3.416	26.10	3.0
0.170	3.424	24.91	2.6

[a] The uncertainty in **a** is ±0.005 Å.
[b] The uncertainty in **c** is ±0.01 Å.
[c] The **c** axis expansion is calculated from the difference between the interlayer spacing for the intercalation compound (**c**/3) and that for TiS_2 (5.7 Å)

the more highly negatively charged TiS_2 layers.

The **a** parameter is sensitive to the degree of charge transfer to the host TiS_2 (*32*). The constant **a** parameter of 3.416 ± 0.002 for $x \leq 0.077$ in Table III indicates that the electron density in the TiS_2 layers is also constant, in agreement with the TGA results. However, the appreciably larger value for $Eu_{0.17}(NH_3)_{0.18}TiS_2$ is probably due to the higher electron density and enhanced electron–electron repulsions in the TiS_2 layers.

3. Magnetic Properties

EPR, magnetization, and magnetic susceptibility measurements have been performed to further elucidate the nature of Eu in these intercalation compounds. Surprisingly, no EPR signals could be observed in the range 4–300 K, even at the highest spectrometer sensitivities. This negative result is consistent with the absence of any $Eu(NH_2)_2$ decomposition product in these compounds, because it has a characteristic EPR signal having a peak-to-peak linewidth of about 1 kG at ambient temperature (*33*). The inability to detect the EPR spectrum of Eu^{3+} is probably due to rapid magnetic relaxation, since this ion is in an orbital F state. Since static magnetic properties are not influenced by dynamical relaxation effects, such measurements should reveal the magnetic species present in these materials.

The temperature dependence of the magnetic susceptibility per mole of Eu for $Eu_x(NH_3)_yTiS_2$ intercalation is displayed in Figs. 3 and 4. At 5 K, the magnetization (M) did not vary linearly with the magnetic field (H), but began to saturate above about 10 kG. The absence of ferromagnetic impurities was demonstrated by the reversibility of the M vs H curve at all temperatures in the range 5–300 K. The Eu contribution to the susceptibility for $x \leq 0.014$ has been extracted by subtracting the susceptibility of $(NH_4^+)_{0.20}TiS_2^{0.20-}$ (*20, 22*) from the measured values. This procedure effectively corrects for the diamagnetism of NH_4^+, the Pauli paramagnetism of the conduction electrons, and the intrinsic as well as impurity paramagnetism of the host TiS_2 (*20*). Corrections for the residual diamagnetism of NH_3 (-15.8×10^{-16} emu/mole NH_3) (*34*) and Eu^{3+} (-20×10^{-6} emu/mole Eu) (*35*), which have not been made, only amounts to about 3% of the measured value for $x = 0.001$ at 30 K. For higher Eu concentrations ($x \geq 0.066$), it is sufficient to substract the susceptibility of TiS_2 from the experimental values, which removes the intrinsic and impurity paramagnetism of TiS_2. The neglected diamagnetism of NH_4^+, NH_3, and Eu^{3+} and the Pauli paramagnetism of the conduction electrons ($\simeq 40 \times 10^{-6}$ emu/mole el) (*20*) are less than 3% of the measured susceptibility at 300 K, and these temperature-independent corrections make even a smaller contribution at lower temperatures.

It is evident in Figs. 3 and 4 that all of the Eu–NH_3 intercalation compounds exhibit Curie-type paramagnetic behavior below about 100 K, with the exception of $Eu_{0.17}(NH_3)_{0.18}TiS_2$. The latter compound has the smallest susceptibility of any of

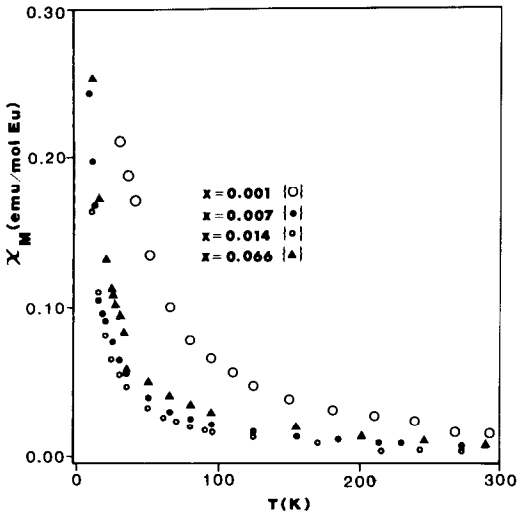

FIG. 3. Magnetic susceptibility per mole of Eu vs temperature for lower Eu concentrations in $Eu_x(NH_3)_y TiS_2$. The susceptibilities for $x \leq 0.014$ and $x > 0.014$ have been corrected for the paramagnetism of $(NH_4^+)_{0.22}TiS_2^{0.22-}$ and TiS_2, respectively.

these compounds over the entire temperature range and displays relatively weak paramagnetic behavior. The observation of such pronounced paramagnetism in almost all of these materials is unexpected if they indeed contain only Eu^{3+}. Eu^{3+} has the electronic configuration $4f^6 4s^2 5p^6$, and the total spin angular momentum of the six unpaired electrons ($S = 3$) is exactly canceled by the total orbital angular momentum ($L = 3$), so that the ground state is nonmagnetic ($J = 0$) and the susceptibility should be independent of temperature within the Russel-Saunders coupling scheme, which should be applicable here. However, the energy difference between the ground state ($J = 0$) and first excited state ($J = 1$) is normally comparable to thermal energy at ambient temperature ($\simeq 200\ cm^{-1}$), so that thermal population of this excited state produces a paramagnetic susceptibility (*36*). Therefore, the susceptibility should be independent of temperature at low temperatures and become paramagnetic at elevated temperatures. This expected behavior is verified by the temperature dependence of the susceptibility for Eu^{3+} in Eu_2CuO_4 depicted in Fig. 5 (*36*).

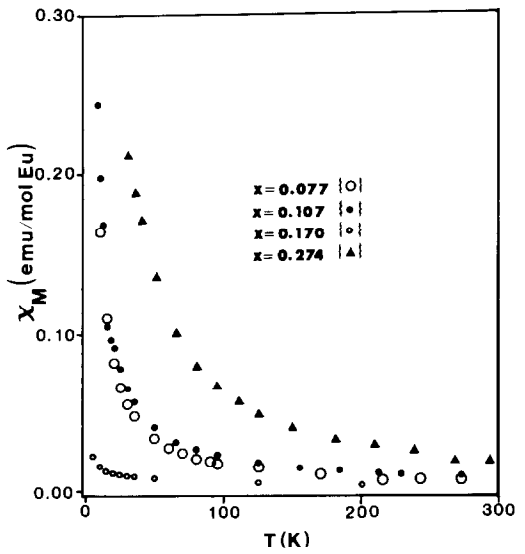

FIG. 4. Magnetic susceptibility per mole of Eu vs temperature for higher Eu concentrations in $Eu_x(NH_3)_y TiS_2$. The susceptibility has been corrected for the paramagnetism of TiS_2.

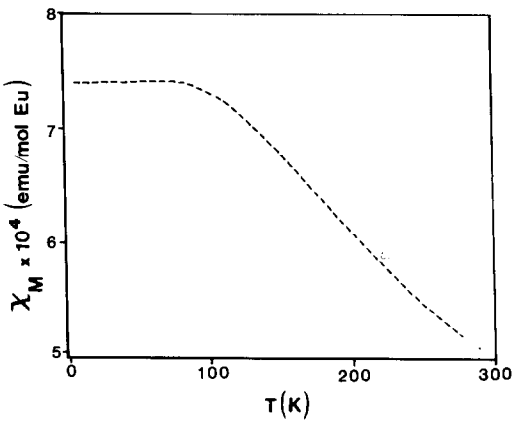

FIG. 5. Temperature dependence of the magnetic susceptibility of Eu_2CuO_4 per mole of Eu^{3+}. From Ref. (*36*).

If Eu^{3+} in $Eu_x(NH_3)_yTiS_2$ exhibits the characteristic type of magnetic behavior illustrated in Fig. 5, then what is the origin of the strong paramagnetism at lower temperatures shown in Figs. 3 and 4? The most obvious secondary paramagnetic species is Eu^{2+}, which has an electronic configuration $4f^75s^25p^6$ and ionic state $^8S_{7/2}$. Since to a good approximation Eu^{2+} is a spin-only S-state ion with long relaxation times, it should be paramagnetic over a wide temperature range, as required. Moreover, the absence of the expected EPR signal for Eu^{2+} (*27, 28*) could originate from rapid electronic exchange between Eu^{2+} and Eu^{3+} via the TiS_2 conduction band, which may result in sufficiently rapid Eu^{2+} spin relaxation to broaden its EPR spectrum beyond observation.

One possible source of Eu^{2+} is that the intercalation compounds are contaminated with $Eu(NH_2)_2$ from decomposition of the Eu–NH_3 solutions, even though the characteristic yellow-orange color of this amide was not observable in the products of our preparations. To investigate the influence of the $Eu(NH_2)_2$ decomposition product on the magnetic properties of these compounds, a sample of $Eu_{0.27}(NH_3)_{0.47}TiS_2$ contaminated with a small amount of $Eu(NH_2)_2$ from decomposition of the Eu–NH_3 solution was prepared and examined. The temperature dependence of the reciprocal susceptibility per mole of Eu for this compound is displayed in Fig. 6. The susceptibility obeys the Curie-Weiss law, and the magnetic moment and Weiss constant, or paramagnetic Curie temperature, are 7.0 β and 5 K, respectively. The $Eu(NH_2)_2$ was observed to order ferromagnetically below about 8 K, which is in reasonable agreement with a Curie temperature of 5.4 K found in previous work (*37*). In addition, for this sample, the EPR spectrum was easily detected and characteristic of $Eu(NH_2)_2$ (*33*), and weak X-ray reflections for $Eu(NH_2)_2$ were observed. Since there was

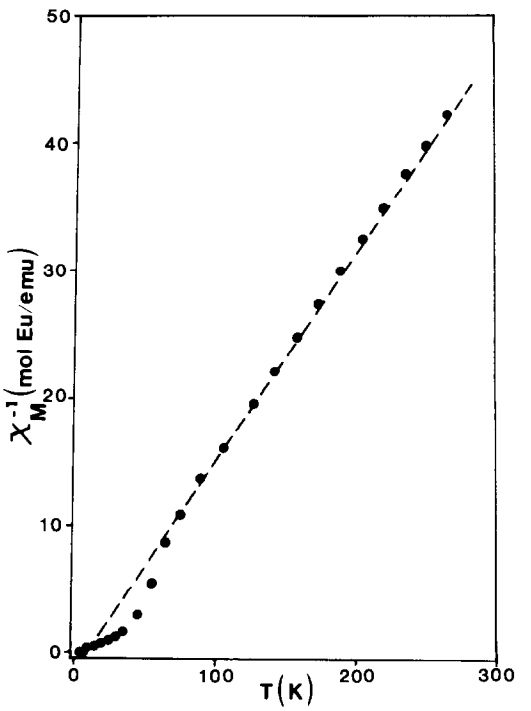

FIG. 6. Reciprocal magnetic susceptibility per mole of Eu vs temperature for $Eu_{0.274}(NH_3)_yTiS_2$ contaminated with a small amount of $Eu(NH_2)_2$.

no evidence of any $Eu(NH_2)_2$ in any of the other intercalation compounds studied, it appears that the Eu^{2+}, if it is indeed present, is not in this form.

Detailed analysis of the magnetic properties of these intercalation compounds provides strong evidence that the secondary paramagnetic species is indeed Eu^{2+}. First, we consider the field dependence of the magnetization. The M vs H curves cannot be fitted to a single Brillouin function having J values characteristic either Eu^{2+} ($J = \frac{7}{2}$) or Eu^{3+} ($J = 0$ with thermal population of $J = 1$) over the entire temperature range. However, quite good agreement can be obtained for an appropriate mixture of Eu^{2+} and Eu^{3+}, as illustrated in Fig. 7, where the M vs H/T curve for $Eu_{0.066}(NH_3)_yTiS_2$ can be fitted quite well to a Brillouin function for a mixture of 30 mol% Eu^{2+} and 70 mol%

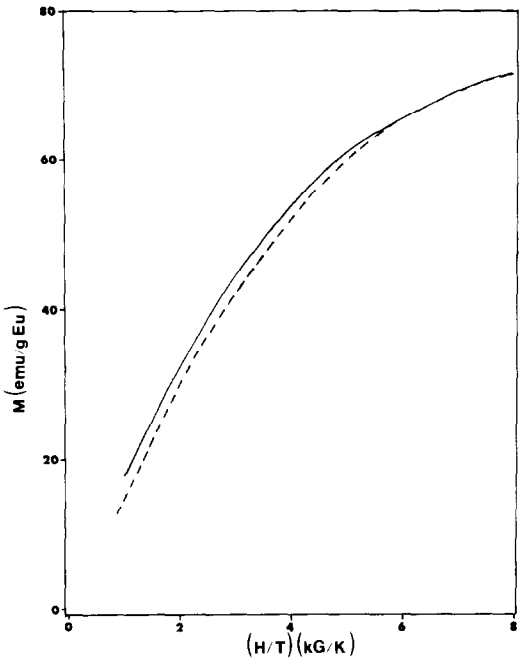

FIG. 7. Comparison of the magnetization vs ratio of magnetic field to temperature for $Eu_{0.066}(NH_3)_yTiS_2$ (solid curve) to that calculated for 30 mol% Eu^{2+} and 70 mol% Eu^{3+} (dashed curve).

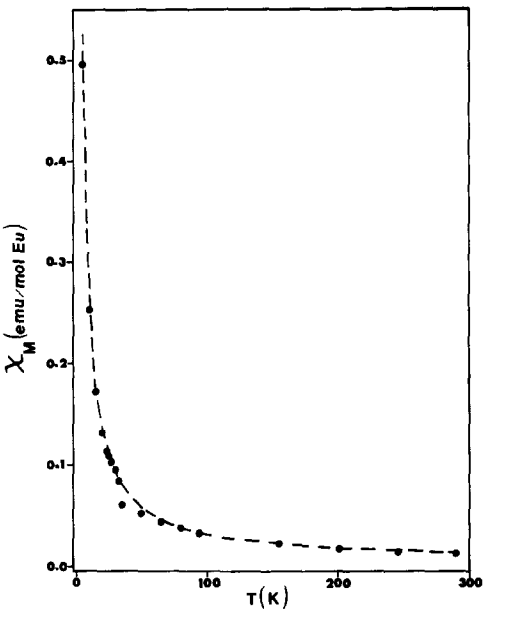

FIG. 8. Comparison of the magnetic susceptibility per mole of Eu vs temperature for $Eu_{0.066}(NH_3)_yTiS_2$ (dots) to that calculated for 33 mol% Eu^{2+} and 67 mol% Eu^{2+} (dashed curve).

Eu^{3+}. It is also possible to determine the relative amounts of Eu^{2+} and Eu^{3+} by fitting the susceptibility calculated for a mixture of Eu^{2+} and Eu^{3+}, $\chi = f\chi(Eu^{2+}) + (1 - f)\chi(Eu^{3+})$, where f is the mole fraction of Eu^{2+}, to the experimental susceptibility, with f being derived from the best least-squares fit. The degree of agreement between the measured and calculated susceptibility for $Eu_{0.006}(NH_3)_yTiS_2$ is shown in Fig. 8. The best fit was obtained for 33 mol% Eu^{2+} and 67 mol% Eu^{3+}, which is in good agreement with the above analysis for the M vs H/T saturation curve. With the exception of $Eu_{0.17}(NH_3)_yTiS_2$, magnetic analyses for the other intercalation compounds yielded similar good agreement between measured susceptibilities and those calculated for a certain relative concentration of Eu^{2+} and Eu^{3+}. Although there is qualitative agreement between experiment and theory for $Eu_{0.017}(NH_3)_yTiS_2$, the measured susceptibility is consistently smaller than the best-fit calculated values, as shown in Fig. 9.

The Eu^{2+} and Eu^{3+} compositions for $Eu_x(NH_3)_yTiS_2$ intercalation compounds derived from magnetic susceptibility measurements are summarized in Table IV. Ex-

TABLE IV

DIVALENT AND TRIVALENT EUROPIUM COMPOSITIONS FOR $Eu_{0.17}(NH_3)_{0.18}TiS_2$ INTERCALATION COMPOUNDS DERIVED FROM MAGNETIC SUSCEPTIBILITY MEASUREMENTS

x	Eu^{2+} (mol%)	Eu^{3+} (mol%)
0.001	≃100	≃0
0.007	22	78
0.014	26	74
0.066	33	67
0.077	18	82
0.107	20	80
0.170	2	98

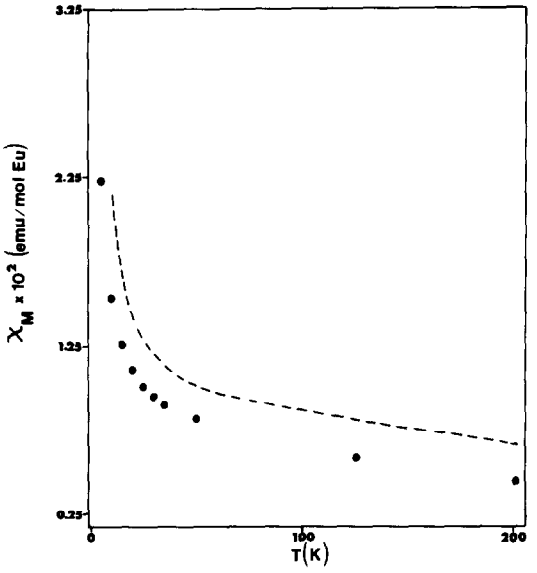

FIG. 9. Comparison of the magnetic susceptibility per mole of Eu vs temperature for $Eu_{0.17}(NH_3)_yTiS_2$ (dots) to that calculated for 2 mol% Eu^{2+} and 98 mol% Eu^{3+} (dashed curve).

cept for $Eu_{0.001}(NH_3)_yTiS_2$, Eu^{3+} is the predominant paramagnetic species in these compounds, with an average of 80 mol% Eu^{3+} and 20 mol% Eu^{2+}. The Eu^{2+} concentration varies from essentially 100 mol% for $Eu_{0.001}(NH_3)_yTiS_2$ to only about 2 mol% for $Eu_{0.17}(NH_3)_yTiS_2$ and is relatively constant for intermediate Eu compositions. This trend is consistent with the known tendency of Eu-NH_3 solutions to decompose very rapidly in the dilute range and to be progressively more stable at higher metallic concentrations (*25, 28*). However, as discussed previously, the decomposition product is not the usual $Eu(NH_2)_2$. Moreover, the appreciable Eu^{2+} concentrations indicates that this cation is intercalated in addition to Eu^{3+}, NH_4^+, and NH_3. An important clue to this enigma is suggested by the results of magnetic analyses of compounds after all the NH_4^+ and NH_3 has been thermally deintercalated at 270°C as indicated by TGA. The results of a typical experiment of this type are shown in Fig. 10, where the temperature dependence of the susceptibility for $Eu_{0.066}(NH_4^+)_{0.06}(NH_3)_{0.26}TiS_2$ and $Eu_{0.066}TiS_2$ are compared. The characterization of the latter compound is described elsewhere. It is evident that the susceptibility of the latter compound has diminished after thermal deintercalation, and detailed magnetic analysis of the data reveals that the Eu^{2+} content has increased from 33 to 52 mol% and the Eu^{3+} concentration has decreased from 67 to 47 mol%, so that 20% of the Eu^{3+} has been reduced to Eu^{2+}. Again, there was no visual, X-ray EPR, or magnetic evidence of any $Eu(NH_2)_2$. Furthermore, we do not anticipate that the high-charge-density Eu^{3+} cation could diffuse rapidly enough at 270°C to the particle edges where its reduction to Eu^{2+} would be effectively catalyzed by exposed Ti, which would require the reduction of roughly ten Eu^{3+} cations to Eu^{2+} per Ti atom if every Ti atom were available at the edges of micrometer-sized particles. These considerations lead us to the

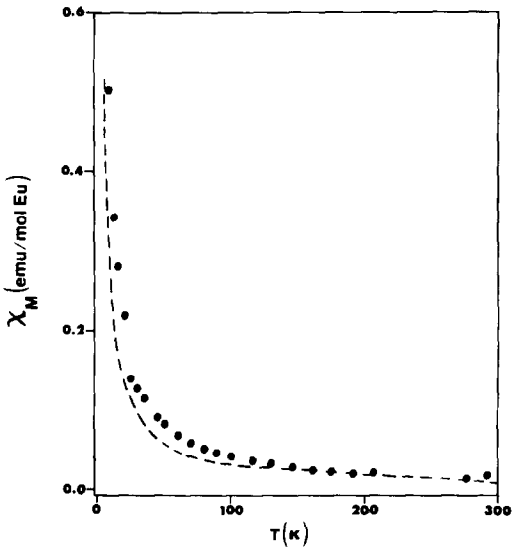

FIG. 10. Comparison of the magnetic susceptibility per mole of Eu vs temperature for $Eu_{0.066}(NH_4^+)_{0.06}(NH_3)_{0.26}TiS_2$ (dashed curve) and $Eu_{0.066}TiS_2$ (dots).

conclusion that the reduction of Eu^{3+} to Eu^{2+} occurs not at the particle edges, but rather in the van der Waals gap. An effective catalyst for this intragap reaction could be the excess intralayer Ti in the host TiS_2, which initially pins the TiS_2 layers together and impedes intercalation (*22*). Indeed, we estimate that the number of intralayer Ti atoms in the starting TiS_2 (≈0.2 mol%) for a 1-μm particle is comparable to the maximum possible number of exposed Ti atoms at the particle edges. The intragap reduction of Eu^{3+} to Eu^{2+} is presumably accompanied by the removal of an equivalent number of electrons for the TiS_2 conduction band. Although the formation of other chemical species, such as amide ions, is conceivable, we have no evidence for their presence. Moreover, electron exchange between Eu^{2+} and Eu^{3+} via the conducting TiS_2 layers cannot explain the reduction of Eu^{3+} to Eu^{2+}, since to a first approximation (i.e., using the rigid-band model and neglecting the change in electron concentration due to deintercalation of NH_4^+), there should be no set change Eu^{2+} and Eu^{3+} concentration after thermal deintercalation of Eu^{2+} and Eu^{3+}. Even if the decrease in conduction-electron density in the TiS_2 layers due to deintercalation of NH_4^+ is considered within the rigid-band model, then one expects some conversion of Eu^{2+} to Eu^{3+}, rather than the reverse, to occur due to the higher electron affinity of the host TiS_2. It should be noted that this same reduction mechanism may well be operative in the formation of the Eu^{2+} originally present in the Eu–NH_3 intercalation compounds, which would explain the absence of $Eu(NH_2)_2$. Since Eu^{2+} can be formed either during or after the intercalation reaction, these compounds are thermodynamically unstable and should be kept at low temperature whenever possible.

Finally, the magnetic effects of the variation in Eu^{2+} and Eu^{3+} compositions in these materials are summarized in Fig. 11, where

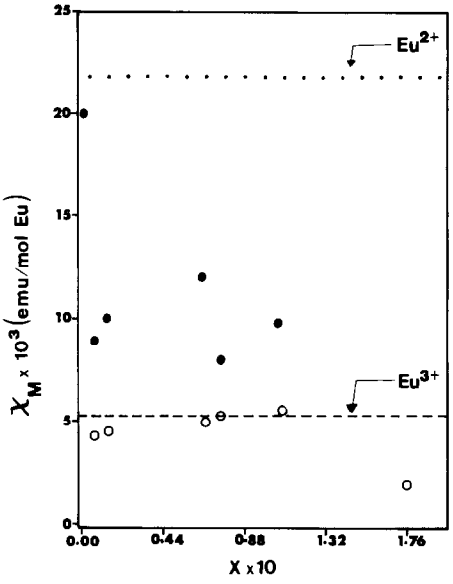

FIG. 11. Comparison of the magnetic susceptibility per mole of Eu at 275 K vs Eu composition for Eu in $Eu_x(NH_3)_yTiS_2$ (dots), Eu^{3+} in $Eu_x(NH_3)_yTiS_2$ (open circles), Eu^{3+} in Eu_2CuO_4 (dashed line), and Eu^{2+} as a free ion (dotted line).

the Eu composition dependence of the susceptibility per mole of Eu at 275 K is shown for Eu in $Eu_x(NH_3)_yTiS_2$, Eu^{3+} in $Eu_x(NH_3)_yTiS_2$ derived from magnetic analyses, Eu^{3+} in Eu_2CuO_4, and Eu^{2+} as a free ion. It is evident that the Eu^{2+}–Eu^{3+} ratio determined from the magnetic analyses used in this study provides a good overall description of the magnetic properties of these complex compounds. The greatest discrepancy occurs for $Eu_{0.17}(NH_3)_yTiS_2$ (see Fig. 9), which is also the most magnetically concentrated compound. The reduced susceptibility compared to that expected for Eu^{3+} suggests that the Eu^{3+} moments may be interacting antiferromagnetically between the layers of this low-dimensional material. Such interactions are plausible because the shortest intraplanar Eu–Eu distances (≈3.4 Å) are considerably shorter than those between layers (≈8.3 Å) and are comparable to those for other Eu com-

pounds that order magnetically (*39–41*). The other more magnetically dilute Eu–NH_3 intercalation compounds show no evidence of magnetic exchange interactions, and their magnetic properties can be understood in terms of noninteracting Eu^{2+} and Eu^{3+} cations.

Conclusions

The results of this study have indicated that the Eu–NH_3 intercalation compounds of TiS_2 are mixed-valence compounds and can be best described by the formulas $(Eu^{3+})_{x'}(Eu^{2+})_{x''}(NH_4^+)_{y'}(NH_3)_{y''}TiS_2^{(3x'+2x''+y')-}$ for $3x' + 2x'' + y' < 0.22$ and $(Eu^{3+})_{x'}(Eu^{2+})_{x''}(NH_3)_{y''}TiS_2^{(3x'+2x'')-}$ for $3x' + 2x'' \geq 0.22$. The intercalation process is complex in the sense that it involves (1) redox reactions producing NH_4^+ until 0.22 ± 0.02 moles el/mol TiS_2 have been transferred to the TiS_2 conduction band, (2) the intercalation of neutral NH_3 after this critical electronic requirement has been satisfied, (3) redox reactions yielding Eu^{3+}, and (4) the formation of Eu^{2+} probably originating from the reduction of Eu^{3+} in the van der Waals gap. The observation of only Eu^{2+} in previous work on the Eu–NH_3 intercalation compounds of NbS_2 and MoS_2 (*25, 26*), if indeed correct, suggests that the electronic structure of the host plays a key role in determining the oxidation state of Eu.

The synthetic, compositional, and structural work reported in this paper has laid the foundation for further investigations of the structure and properties of these intercalation compounds. Future search will be focused on comparable studies of magnetically more concentrated compounds as well as Mössbauer spectroscopy to further elucidate the nature of the magnetic interactions and the Eu site symmetry in these materials.

Acknowledgments

The authors acknowledge the use of instrumentation within the X-ray Diffraction Facility and Magnetism and Magnetic Resonance Facility at Arizona State University.

References

1. F. R. GAMBLE AND T. H. GEBALLE, *in* "Treatise on Solid State Chemistry" (N. B. Hannay, Ed.), Vol. 3, p.89, Plenum, New York, 1974.
2. M. S. WHITTINGHAM, *Prog. Solid State Chem.* **12,** 41 (1978).
3. F. A. LEVY (Ed.), "Intercalated Layered Materials," Reidel, Dordrecht, 1979.
4. M. S. WHITTINGHAM, *J. Solid State Chem.* **29,** 303 (1979).
5. H. TRIBUTSCH, *J. Electrochem. Soc.* **125,** 1086 (1978).
6. G. W. STUPIAN AND P. COSSE, *J. Vac. Sci. Technol.* **13,** 684 (1976).
7. A. L. FARRAGHER AND P. CASSE, *Catal. Prog. Int. Congr. 5th 2,* 3101 (1972).
8. P. GRANGE AND B. DELMON, *J. Less-Common Met.* **36,** 353 (1974).
9. F. R. GAMBLE, J. H. OSIECHI, M. CAIS, R. PICHARODY, F. J. DISALVO, AND T. H. GEBELLE, *Science* **174,** 493 (1971).
10. B. G. SILBERNAGEL AND F. R. GAMBLE, *Phys. Rev. Lett.* **32,** 1436 (1974).
11. R. R. CHIANELLI, J. C. SCANLON, M. S. WHITTINGHAM, AND F. R. GAMBLE, *Inorg. Chem.* **14,** 1691 (1975).
12. M. B. DINES, *J. Chem. Soc. Chem. Commun.,* 220 (1975).
13. M. B. DINES AND R. B. LEVY, *J. Phys. Chem.* **29,** 1979 (1975).
14. B. G. SIBERNAGEL, M. B. DINES, F. R. GAMBLE, L. A. GEBBAARD, AND M. S. WHITTINGHAM, *J. Chem. Phys.* **65,** 1906 (1976).
15. B. G. SILBERNAGEL AND F. R. GAMBLE, *J. Chem. Phys.* **65,** 1914 (1976).
16. R. SCHÖLLHORN AND H. D. ZAGEFKA, *Angew. Chem. Int. Ed. Engl.* **16,** 199 (1977).
17. H. T. WEAVER, J. E. SCHIRBER, AND B. G. SILBERNAGEL, *Solid State Commun.* **28,** 21 (1978).
18. G. V. SUBBA RAO AND M. W. SHAFER, *in* "Intercalated Layered Materials" (F. Levy, Ed.), p. 99, Reidel, Dordrecht, 1979.
19. C. REIKEL, R. SCHÖLLHORN, AND J. TOMKINSON, *Z. Naturforsch A* **35,** 590 (1980).
20. L. BERNARD, M. MCKELVY, W. GLAUNSINGER, AND P. COLOMBET, *Solid State Ionics* **15,** 301 (1985).

21. L. BERNARD, W. GLAUNSINGER, AND P. COLOMBET, *Solid State Ionics* **17,** 81 (1985).
22. M. J. MCKELVY, PH.D. THESIS, Arizona State University, 1985.
23. S. P. HSU, PH.D. THESIS, Arizona State University, 1985.
24. M. J. MCKELVY AND W. S. GLAUNSINGER, *J. Solid State Chem.*, **67,** 143 (1987).
25. G. V. SUBBA RAO, M. W. SHAFER, AND L. J. TAO, *AIP Conf. Proc., AM. Inst. of Phys., N.Y.* **10,** 1173 (1973).
26. G. V. SUBBA RAO, M. W. SHAFER, AND L. J. TAO, *Mater. Res. Bull.* **8,** 1231 (1973).
27. F. Y. ROBB, T. R. WHITE, AND W. S. GLAUNSINGER, *J. Magn. Reson.* **48,** 382 (1982).
28. S. P. HSU, C. B. ZIMM, AND W. S. GLAUNSINGER, *J. Solid State Chem.* **54,** 346 (1984).
29. A. H. THOMPSON, F. R. GAMBLE, AND C. R. SYMON, *Mater. Res. Bull.* **10,** 915 (1975).
30. K. JONES, *in* "Comprehensive Inorganic Chemistry" (J. C. Bailar *et al.*, Eds.), Vol. 2, p. 244, Pergamon, Elmsford, NY, 1974.
31. This value is derived by taking one-half the nearest-neighbor distance in solid NH_3. The NH_3 radius estimated from the van der Waals radii of N and H is approximately 1.6 Å.
32. M. S. WHITTINGHAM AND A. H. THOMPSON, *J. Chem. Phys.* **62,** 1588 (1975).
33. G. F. KOKOSZKA AND N. J. MAMMANO, *J. Solid State Chem.* **1,** 227 (1970).
34. W. S. GLAUNSINGER, S. ZOLOTOV, AND M. J. SIENKO, *J. Chem. Phys.* **56,** 4756 (1972).
35. P. W. SELWOOD, "Magnetochemistry," 2nd ed., Interscience, New York, 1956.
36. R. SAEZ PUCHE, M. NORTON, T. R. WHITE, AND W. S. GLAUNSINGER, *J. Solid State Chem.* **50,** 281 (1983).
37. F. HULLIGER, *Solid State Commun.* **8,** 1477 (1970).
38. S. P. HSU AND W. S. GLAUNSINGER, *Mater. Res. Bull.*, **21,** 1063–1072 (1986).
39. H. H. WICKMAN AND E. CATALANO, *J. Appl. Phys.* **39,** 1248 (1968).
40. T. KASUYA, IBM *J. Res. Dev.* **14,** 214 (1970).
41. G. GROLL, *Z. Phys.* **243,** 60 (1971).